Microelectronic Engineering 111 (2013) 105–109

Contents lists available at SciVerse ScienceDirect

Microelectronic Engineering

journal homepage: www.elsevier.com/locate/mee

An ultraviolet sensor using spin–coated ZnO nanoparticles based on surface acoustic waves

Ki Jung Lee, Haekwan Oh, Minuk Jo, Keekeun Lee, Sang Sik Yang *

Department of Electrical and Computer Engineering, Ajou University, Woncheon-dong, Yeongtong-gu, Suwon 443-749, Republic of Korea

ARTICLE INFO

Article history:
Available online 24 February 2013

Keywords:
Ultraviolet sensor
ZnO nanoparticles
Surface acoustic wave

ABSTRACT

This paper proposes an ultraviolet (UV) sensor based on surface acoustic waves (SAWs) using ZnO nanoparticles. The UV sensor consists of an UV-sensitive film and a piezoelectric substrate propagating shear–horizontal (SH) waves. The UV-sensitive film is fabricated using commercially available ZnO nanoparticles by a solution process. The material properties of the ZnO nanoparticle-based film were evaluated using scanning electron microscopy, photospectrometry, and X-ray diffraction. The characteristics of the SAW-based UV sensor were tested under UV light (λ = 365 nm) using a network analyzer and a commercial UV lamp. The sensitivity and the linearity of the SAW-based UV sensor are 180.43 Hz/μW and 0.932 in frequency shift and 0.14°/μW and 0.965 in phase shift, respectively. The fabrication of the newly developed SAW-based UV sensor is simple but shows comparable characteristics to sensors having a much more complex production process.

1. Introduction

Recently, ultraviolet (UV) detection is applied in many areas such as astronomy, polymer resin curing, combustion engineering, water purification, flame sensing, secure space-to-space communications, biological sensing, and pollution monitoring. For an UV detector, wide-bandgap semiconductors are commonly used. Zinc oxide (ZnO) is an n-type semiconducting oxide material used in many applications, including transparent conducting electrodes, gas sensors, and optoelectronic devices. ZnO has an exciton binding energy of 60 meV, a large bandgap (E_g) of ~3.3 eV, and is transparent in the visible wavelength range. Moreover, ZnO is chemically stable and can be applied in harsh environments such as at high temperatures. ZnO is a promising material for UV detection owing to its simple production through thin film fabrication process, its excellent radiation hardness, and the superiority of its UV radiation detection [1–10]. In general, many UV detectors based on metal–photoconductive semiconductor–metal structures have been frequently investigated, and UV sensors using ZnO as the UV-sensitive material have already been reported [1,3–10]. Researchers generally measure the change in the photocurrent or photovoltage of the UV sensor in the presence or absence of UV illumination to investigate the performance of UV sensors [7–9]. It is necessary to use complex measurement systems for detecting a minute change in the photocurrent or photovoltage. Alternatively, Qiu et al. developed a film bulk acoustic wave resonator (FBAR)-based UV sensor using a ZnO film, and they observed a frequency upshift of 9.8 kHz at an UV intensity of 600 μW/cm^2 [2].

Surface acoustic wave (SAW)-based sensors are highly sensitive, fabricated easily using microelectromechanical systems (MEMS) technique, and enable readout in the frequency domain. Therefore, they do not require complicated instruments for measurement and are capable of wireless sensing for remote measurement applications. Furthermore, SAW-based devices have the advantage of passive operation, which is essential for low power consumption. Kumar et al. presented a SAW-based UV sensor with a ZnO film deposited by a magnetron sputtering technique and capable of detecting an UV light intensity of 450 nW/cm^2. They observed a frequency downshift of ~28 kHz on an UV illumination of ~34 μW/cm^2 [5]. In this paper, we propose a SAW-based UV sensor which harnesses the acousto-electric interaction between electric fields generated on a piezoelectric substrate by SAW and the photoconductivity of the ZnO film. The device is composed of a ZnO film as the photosensitive layer and $LiNbO_3$ as the piezoelectric substrate. The ZnO film was deposited using a solution process with commercial ZnO nanoparticles (NPs). Only few researches on photodetectors employing ZnO NPs have been reported so far. The NP-based structure would enhance the light absorption efficiency of ZnO considerably compared to other structures. In addition, NP-based devices can be fabricated simply by a solution process [6,8]. The fabrication technique via the solution process has advantages such as simplicity, possibility of producing large-area, scope for mass production, and low cost. To minimize damping effects of the ZnO film and to decrease insertion loss of the sensor, 41° YX

* Corresponding authors. Tel.: +82 31 219 2488; fax: +82 31 212 9531.
E-mail address: ssyang@ajou.ac.kr (S.S. Yang).

0167-9317/$ - see front matter © 2013 Elsevier B.V. All rights reserved.
http://dx.doi.org/10.1016/j.mee.2013.02.025

$LiNbO_3$, which propagates the shear-horizontal (SH) mode of SAW, was used as the piezoelectric substrate.

2. Operation principle

2.1. UV response of ZnO NP-based film

Two processes affect the detection of UV radiation using ZnO NP-based films. One involves surface-adsorbed species, and the other is a volume process [7]. UV detection is mainly governed by the generation of excitons consisting of electron–hole (e^-–h^+) pairs with energies higher than the bandgap of ZnO NPs under irradiation. In an atmosphere without UV light, oxygen molecules, which play an important role in UV detection, are adsorbed onto the surface of the ZnO NP-based film. These captured oxygen molecules are deprived of free electrons on the ZnO NP-based film and induce a depletion region, leading to a reduction in the ZnO conductivity and the formation of oxygen ions such as O_2^-, O^-, or O^{2-} on the surface.

$$\begin{aligned} &O_2(g) \leftrightarrow O_2(ad), O_2(ad) + e^- \rightarrow O_2^-(ad), \\ &O_2^-(ad) + e^- \rightarrow O_2^{2-}(ad) \rightarrow 2O^-(ad), \\ &1/2O_2 + e^- \rightarrow O^-(ad), or 1/2O_2 + 2e^- \rightarrow O^{2-}(ad). \end{aligned} \tag{1}$$

UV photons have a higher energy than the bandgap energy of ZnO NPs, thus generating e^-–h^+ pairs. The photogenerated holes migrate to the ZnO NP surface and react with negatively charged adsorbed oxygen ions, thereby causing a narrowing of the depletion region of the ZnO NP-based film.

$$\begin{aligned} &H^+ + O_2^-(ad) \rightarrow O_2(g), h^+ + O^-(ad) \rightarrow 1/2O_2, or \\ &2h^+ + O^{2-}(ad) \rightarrow 1/2O_2. \end{aligned} \tag{2}$$

Neutralized oxygen molecules are desorbed from the surface, and the photogenerated free electrons flow through the film. This causes an increase in the concentration of electrons. Consequently, the photodesorbed oxygen molecules and the photogenerated free electrons contribute to an increase in the conductivity of the ZnO NP-based film by reducing the electron depletion region and electrical resistance. This photodesorbtion process greatly increases the conductivity of the ZnO NP-based film. When the UV light is turned off, the captured oxygen molecules at the surface, which are now deprived of free electrons, reduce the conductivity of the film [1,7–9].

2.2. Principle of a SAW-based UV sensor

Fig. 1 shows the construction scheme of the proposed SAW-based UV sensor. It is composed of three different layers: (1) the ZnO NP-based film, (2) a metal layer for interdigital transducers (IDTs), and (3) a piezoelectric substrate. The suggested device operates by the acousto-electric interaction between the electric fields generated on a piezoelectric substrate by SAW and the photoconductivity of the ZnO film. On applying power to the input, the SAW propagates from the input IDT to the output IDT along the surface of the piezoelectric substrate. The SAW propagation velocity is determined by the piezoelectric substrate and parameters of the overlaying film, such as mass, elastic modulus, and conductivity. As mentioned earlier, the conductivity of ZnO NP-based films increases under UV irradiation. Then, the acousto-electric interactions change the SAW velocity, which results in a phase shift. The change in the SAW velocity, Δv due to the acousto-electric interaction is described by Eq. (3).

$$\frac{\Delta v}{v_0} = \frac{K^2}{2} \frac{1}{1 + (\sigma/\sigma_m)^2} \tag{3}$$

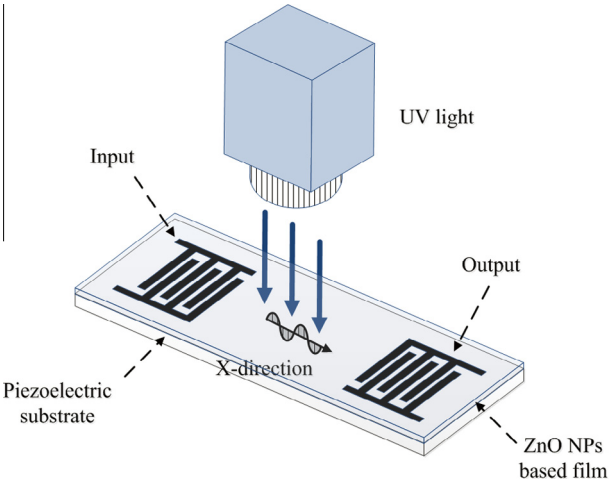

Fig. 1. The construction scheme of the proposed SAW-based UV sensor.

K^2, v_0, σ, and σ_m are the coupling coefficient, the SAW velocity on a free surface, the sheet conductivity, and a material constant, respectively [3–6,10]. The difference in the SAW velocity causes a frequency shift. Therefore, we investigate this frequency shift due to UV irradiation to evaluate the performance of the proposed SAW-based UV sensor.

3. Design and fabrication

ZnO is a well-known semiconducting oxide material and has been actively researched for many decades. Its material properties have been investigated in a number of reports. In optoelectronic applications, ZnO has some advantages such as a large exciton binding energy and a direct wide-bandgap. In particular, owing to its bandgap of 3.3 eV, it is transparent in the visible wavelength range, and therefore, it is suitable as an UV-sensitive material. There are several methods for growing ZnO films such as chemical-vapor transport, vapor-phase growth, hydrothermal growth, and sputtering. These methods require stringent control over ambient conditions such as size, temperature, and vacuum pressure. ZnO NPs, however, can be deposited simply by spin-coating. This method has advantages such as simplicity, possibility of producing large-area, scope for mass production, and low cost. As previously stated, the UV response of ZnO is related to its surface area. This means that if the UV-sensitive area is increased, the sensitivity can be enhanced.

A 41° YX $LiNbO_3$ was employed as the piezoelectric substrate. S. Kumar reported that a 71 nm–thick ZnO overlayer was a suitable film for UV sensing based on Rayleigh waves and no mass loading effect was evident in the frequency spectrum of the ZnO/$LiNbO_3$ SAW device [5]. It, however, was too thin to adsorb UV photons sufficiently under illumination. The penetration depth of UV photons in wide bandgap semiconductor is around 200–250 nm [9]. In this paper, the thickness of the UV–sensitive ZnO film is 300 nm which has not only an effective absorption of UV photons but also a high damping effect on Rayleigh waves. Therefore, we decided to use a 41° YX $LiNbO_3$ substrate as it propagates such SH wave, thereby minimizing the damping effect of the ZnO film and decreasing the insertion loss of the multi–layered sensor. Also, a high electromechanical coupling coefficient (K^2 = 17.2) of the substrate would results in a high sensitivity of the sensor, because a higher electromechanical coupling coefficient leads to a greater SAW velocity variation. The properties of the 41° YX $LiNbO_3$ substrates are listed in Table 1.

Table 1

Piezoelectric substrate	41° YX $LiNbO_3$
SAW velocity in *x*-axis (m/s)	4792
Electromechanical coupling coefficient K^2 (%)	17.2
Temperature coefficient of delay (ppm/°C)	80

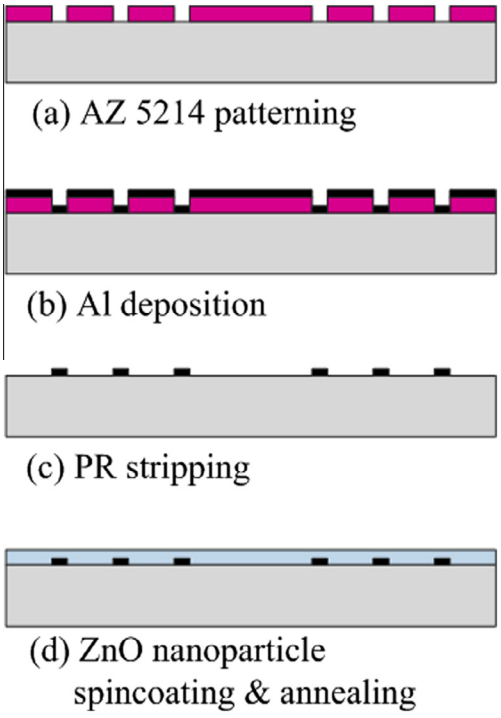

Fig. 2. The fabrication procedure of the SAW-based UV sensor.

The fabrication process of the SAW-based UV sensor is shown in Fig. 2. A 41° YX $LiNbO_3$ wafer was cleaned with acetone and methanol and rinsed in deionized (DI) water. A lift-off process was applied for the IDT structures. For this, a 1 μm thick photoresist (PR, AZ5214E, Clariant Co.) was spin-coated, exposed, and developed for the 2 IDT patterns. Then, aluminum with a thickness of 150 nm was deposited onto the patterned 41° YX $LiNbO_3$ substrate using an electron beam evaporator. The remaining PR on the substrate was then removed by immersion into AZ 400T, a positive PR stripper, leaving aluminum IDT patterns. The wafer was subsequently cleaned by rinsing several times with DI water. After that, the commercial ZnO NPs (NanoShield ZN-3010, Alfa Aesar) were spin-coated onto the substrate and annealed in a box furnace at 300 °C in air. The thickness of the spin–coated ZnO NP–based film measured with a surface profiler (NanoMap 500LS, AEP technology) is approximately 300 nm.

4. Experimental

The optical image of the fabricated SAW-based UV sensor is shown in Fig. 3(a). The diced device was mounted on a printed circuit board (PCB) with bonded gold wires for electrical connection. The size of the fabricated device was 22.0 × 11.5 mm^2.

4.1. ZnO NP-based thin film

To examine the ZnO NP-based film, samples for scanning electron microscopy (SEM), photospectrometry, and X-ray diffraction (XRD) were prepared by the same fabrication process on Pyrex glass. A SEM image of the ZnO NP-based film is shown in Fig. 3(b). As can be seen, the size of the ZnO NPs is in the range of some tens to a few hundreds of nanometers, and their average size was approximately 70 nm. We could also observe some voids on the surface of the film. This caused a nonuniform surface of the film and maximized the UV-reactive surface area, and hence, it was

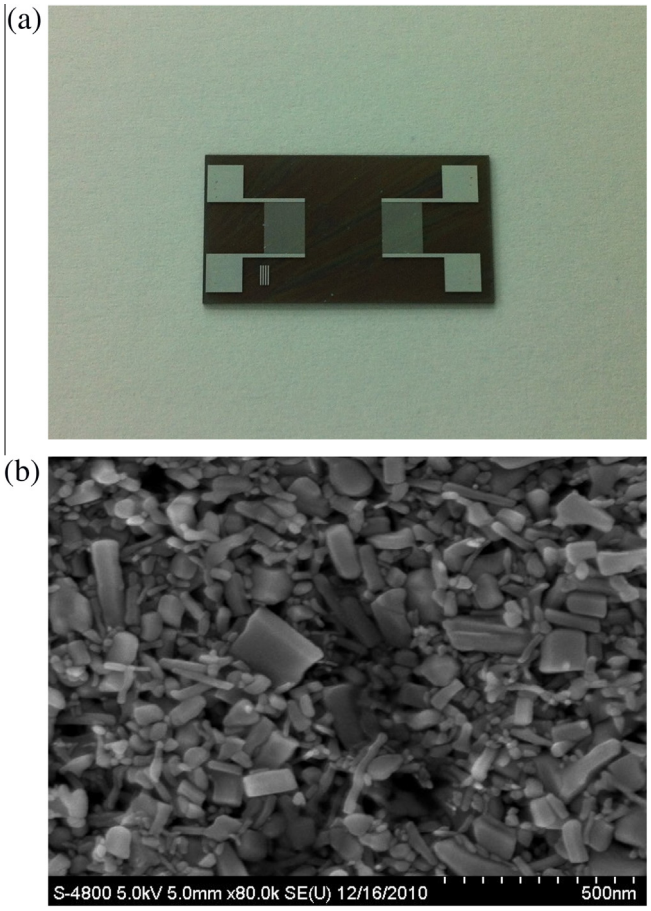

Fig. 3. (a) The optical image of the fabricated device and (b) the SEM image of a ZnO NP-based film on the $LiNbO_3$ substrate.

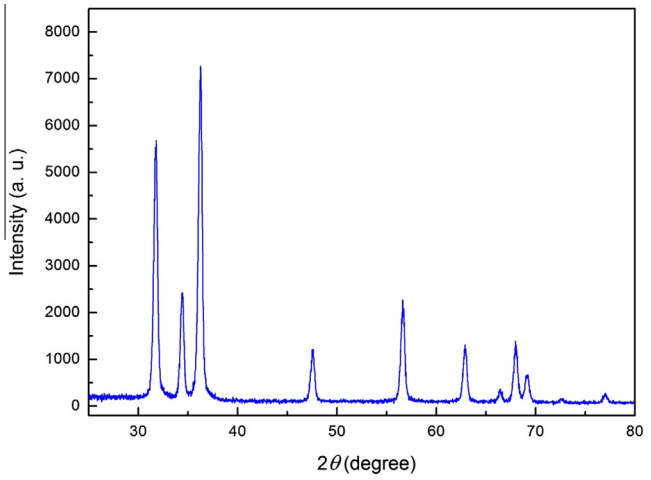

Fig. 4. The results of XRD pattern of the ZnO NP-based film annealed at 300 °C in air.

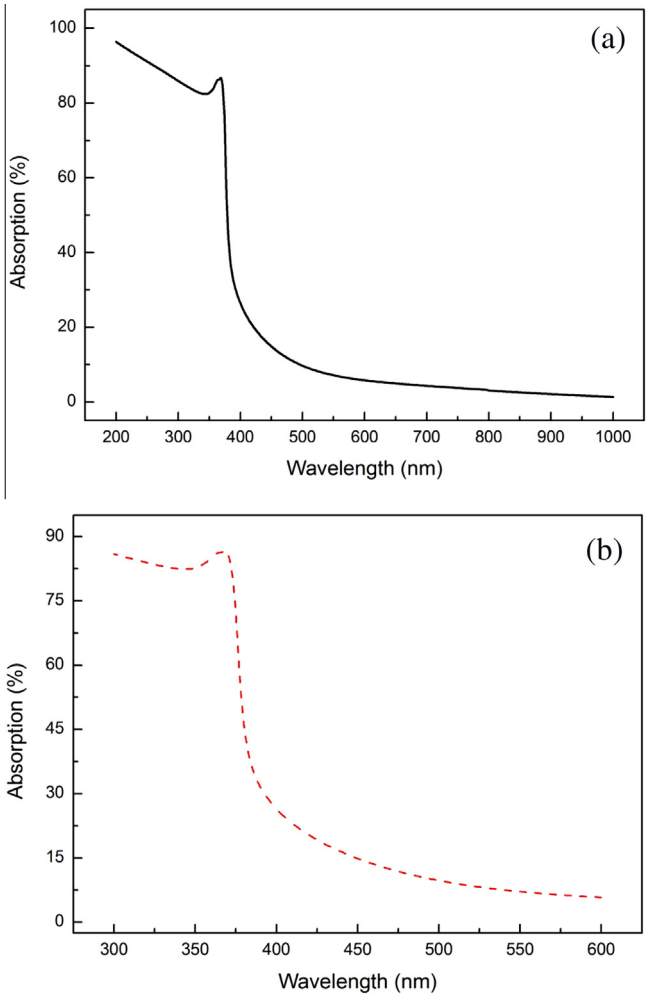

Fig. 5. The photospectrometer measurements of the ZnO NP-based film for the wavelength ranging (a) from 200 to 1000 nm and (b) from 300 to 600 nm, respectively.

expected that the UV sensitivity would be increased. XRD analysis was performed to compare the ZnO NP-based film with ZnO films grown as bulk crystals. The XRD pattern of the ZnO NP-based film fabricated by an aqueous solution process on a glass substrate is depicted in Fig. 4. This plot shows relatively sharp peaks (100), (002), (101), and (110) of the corresponding ZnO structure, and reflects the polycrystalline characteristics of the material. Fig. 5 shows the spectral response of the ZnO NP-based film in different wavelength regions. The relative spectral response, measured in the wavelength range 200–1000 nm, is shown in Fig. 5(a). The maximum UV absorption of the ZnO NP-based film was observed in the wavelength range 200–400 nm, and the absorption peak related to the bandgap energy of ZnO was reached at 350–370 nm. Fig. 5(b) shows the part of the spectral response in the wavelength range 300–600 nm. A sharp adsorption peak is seen at about 370 nm, which is consistent with the bandgap of ZnO and shows that a ZnO NP-based film is suitable for use as the UV detector.

To examine the UV response of the ZnO NP-based film, the photocurrent excited by UV irradiation was measured using a commercial UV lamp and a semiconductor parameter analyzer type HP 4155C. The UV intensity was determined by controlling the distance between the SAW-based UV sensor and the UV lamp and measured with a commercial UV intensity meter. The *I–V* curves of the photocurrent under irradiation of 365 nm light (corresponding to the ZnO bandgap) at an intensity of 300 μW/cm^2 and the

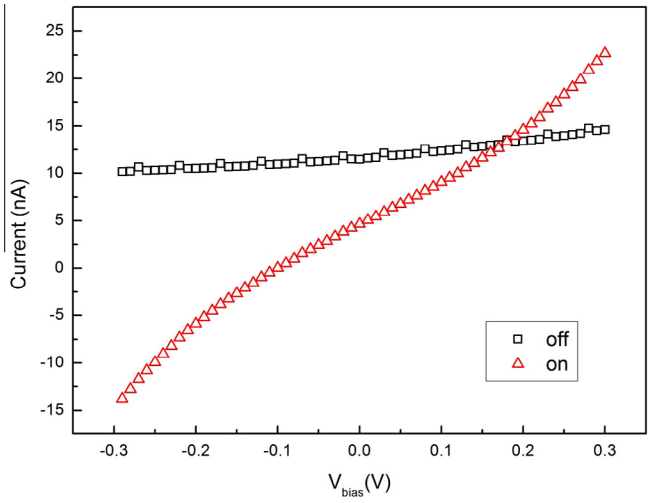

Fig. 6. The *I–V* curves of the ZnO NP-based film with UV (wavelength of 365 nm and intensity of 300 μW/cm^2) illumination turned on and off.

dark current are plotted in Fig. 6. Both *I–V* curves show nearly ohmic characteristics. The plot demonstrates that the photocurrent of the ZnO NP-based film was amounted to 22.67 nA at 0.3 V under 365 nm irradiation and that of the dark current was as low as 14.64 nA at 0.3 V, implying a low ratio of the photocurrent to the dark current (on/off ratio). However, the slope of the *I–V* curve of the ZnO NPs exposed to 365 nm light was about 7 times greater than that of the dark current, which is not a negligible value. Thus, these results indicated that the conductivity of the ZnO NP-based film is increased linearly under increasing UV intensity.

4.2. ZnO NP-based UV SAW sensor

The experimental setup is shown in Fig. 7. Using the HP 8753ES network analyzer, we measured the frequency and phase response of the SAW delay lines. Fig. 8 shows the frequency response of S_{21} of the fabricated device with an insertion loss and a center frequency of about 27 dB and 234.8 MHz, respectively. An experiment for device characterization was carried out using a commercial UV lamp and a network analyzer in the clean room maintained constant temperature of 20 °C and humidity of 40%. The frequency and the phase shifts of the SAW-based UV sensor exposed to UV light (λ = 365 nm) for various intensities ranging from 40 to 430 μW/cm^2 is shown in Fig. 9. No temperature change of the

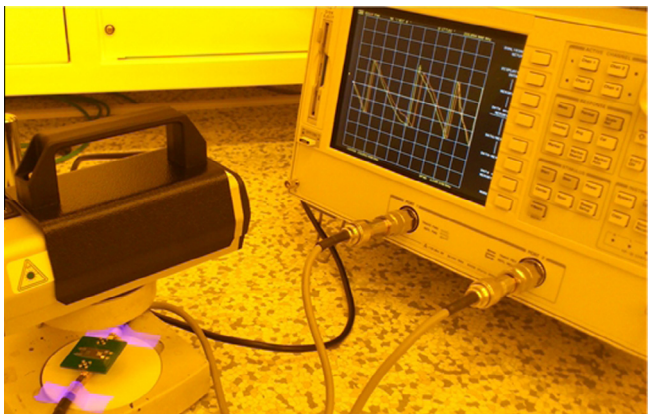

Fig. 7. Photograph of the experimental setup for the characterization of the fabricated device.

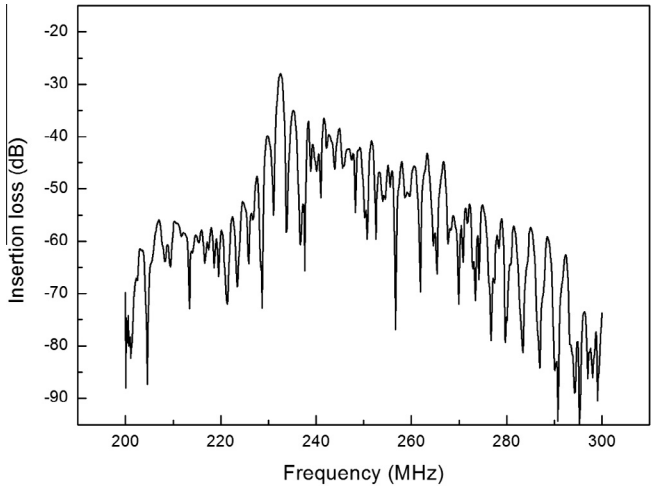

Fig. 8. The frequency response of S_{21} for the fabricated ZnO NP-based SAW device measured with UV light turned off.

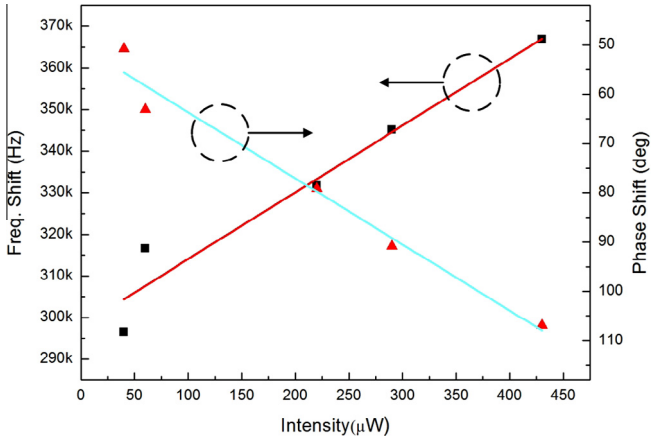

Fig. 9. The frequency shift (left Y) and the phase shift (right Y) for various intensities of UV light with the wavelength of 365 nm.

SAW device exposed to UV light within this intensity range was observed. As expected, free electrons were generated in the ZnO NP-based film under UV illumination, and the interaction between the SAW and the conductivity of the film caused an SAW velocity change. According to Eq. (3), as the conductivity of the film increases, the SAW velocity decreases leading to the frequency and the phase shift. The UV sensor based on SAWs showed a frequency shift of 366.92 kHz and a phase shift of 106.88° at an UV light intensity of 430 μW/cm^2. The sensitivity and the linearity of the SAW-based UV sensor were 180.43 Hz/μW and 0.932 in frequency shift and 0.14°/μW and 0.965 in phase shift, respectively. Although, the device detected a low intensity of UV light, the response of the proposed SAW-based UV sensor at UV intensities below 40 μW/cm^2 could not be measured due to the limitations of the experimental instruments.

5. Conclusion

The realization of a ZnO NP-based UV SAW sensor was demonstrated. Although this sensor was fabricated by a solution process, it shows good characteristics of UV sensitivity, as compared to UV sensors fabricated by high-cost ZnO film deposition. The spectral response of the ZnO NP-based film indicates that it is suitable for the UV detection. The characteristics of the *I–V* curves prove that excitons contribute to the photocurrent generation under UV irradiation and enhance the conductivity of the film, thereby leading to a velocity change in the SAWs. The *I–V* characteristics show that the on/off ratio was about 1.5 at 0.3 V. Although this is not a high value, a maximum of 336.92 kHz in frequency shift and 106.88° in phase shift of the SAW was observed at UV light intensity of 430 μW/cm^2. The sensitivity and the linearity of the SAW-based UV sensor are 180.43 Hz/μW and 0.932 in frequency shift and 0.14°/μW and 0.965 in phase shift, respectively. Despite the device is not optimized, it shows a good sensitivity and linearity. In case of a conductivity change in the ZnO NP-based film, the fall time is below one second, but it takes several minutes to rise to the steady state. We believe that a lagging response time originates from the large total area of the device, because the reaction surface is an important parameter to UV detection. Reducing the size of the reaction area is expected to enhance the response time. As a future work, the optimization of the design of the device and the treatment of the ZnO NP-based film will be studied. We will carry out an experiment on low-level UV light detection with improved experimental instruments.

Acknowledgements

This work was supported by the National Research Foundation of Korea (NRF) grant funded by the Korea government (MEST) (No. 2009-0081200).

References

[1] X. Qiu, J. Zhu, J. Oiler, C. Yu, Z. Wang, H. Yu, Applied Physics letters 94 (2009) 151917.
[2] U. Ozgur, Ya.I. Alivov, C. Liu, A. Teke, M.A. Reshchikov, S. Dogan, V. Avrutin, S.-J. Cho, H. Morkoc, Journal of Applied Physics 98 (2005) 041301.
[3] S. Kumar, G. Kim, K. Sreenivas, R. Tandon, Journal of Electroceramics 22 (2003) 198–202.
[4] P. Sharma, K. Sreenivas, Applied Physics letters 83 (2003) 3617–3619.
[5] S. Kumar, P. Sharma, K. Sreenivas, Semiconductor Science and Technology 20 (2005) L27–L30.
[6] H. Oh, K. Lee, H. Jung, S. Yang, K. Lee, Proceeding of KMEMS (2012) 475–476.
[7] O. Lupan, L. Chow, G. Chai, Sensors and Actuators B: Chemical 141 (2009) 511–517.
[8] J. Jun, H. Seong, K. Cho, B. Moon, S. Kim, Ceramics International 35 (2009) 2797–2801.
[9] H. Yadav, K. Sreenivas, V. Gupta, Journal of Applied Physics 107 (2010) 044507.
[10] N. Emanetoglu, J. Zhu, Y. Chen, J. Zhong, Y. Lu, Applied Physics Letters 85 (2004) 3702–3704.